

## A SOFC based on a co-ionic electrolyte

A. Demin<sup>a</sup>, P. Tsiakaras<sup>b,\*</sup>, E. Gorbova<sup>a</sup>, S. Hramova<sup>a</sup>

<sup>a</sup> Institute of High Temperature Electrochemistry RAS, 22 S. Kovalevskoy, 620219 Ekateriburg, Russia

<sup>b</sup> Department of Mechanical and Industrial Engineering, University of Thessaly, Pedion Areos, 38334 Volos, Greece

Received 30 September 2003; accepted 13 October 2003

### Abstract

In the present work the operation of a SOFC based on a co-ionic electrolyte is considered. The special case of ion transport in a co-ionic electrolyte is analyzed. It is shown that partial ion currents do not correspond to ion transfer numbers, a partial proton current being higher than a proton transfer number under the working conditions of the SOFC. It is shown that both fuel utilization and electric efficiency are higher when the proton transfer number is higher. It is established that the maximum achievable efficiency of a hydrogen-fed SOFC based on the co-ionic electrolyte with  $t_H = 0.5$  is 0.78 at 900 K whereas the efficiency is 0.62 when the SOFC works at 70% of its maximum power. © 2004 Elsevier B.V. All rights reserved.

**Keywords:** SOFC; Co-ionic electrolytes

### 1. Introduction

Solid oxide fuel cells (SOFCs) are considered as one of the most promising electric generators. At the initial stage, a SOFC based on an oxygen ion electrolyte, SOFC(O<sup>2-</sup>), has been developed. During the last two decades however, a lot of oxides possessing proton conduction have been discovered [1]. They were called “proton conductors” or “proton electrolytes”. Some of them have purely proton conduction, but the majority have both proton and oxygen ion conduction. They can be called “co-ionic electrolytes” [2] and characterized by a proton transfer number,  $t_H$ , which is usually measured in “one-chamber” conditions [3].

Theoretical analysis showed that a SOFC based on a pure proton electrolyte, SOFC(H<sup>+</sup>), can reach considerably higher efficiency than the SOFC(O<sup>2-</sup>) [4]. It is of theoretical and practical interest to study the influence of the proton transfer number on efficiency and other characteristics of the SOFC based on a co-ionic electrolyte, called hereafter SOFC(O<sup>2-</sup>, H<sup>+</sup>).

### 2. Theoretical model

A co-ionic-electrolyte-based cell and its equivalent circuit are presented in Fig. 1. Here it is assumed that oxidant is

at the left side and fuel is at the right side of the cell. It is assumed that  $R_i = R/t_i$ , where  $R$  is ohmic resistance of the electrolyte,  $t_i$  is corresponding ion transfer number. Electromotive forces corresponding to each kind of charge carrier are calculated by equations

$$E_0 = -\frac{RT}{4F} \ln \frac{p''O_2}{p'O_2}, \quad (1)$$

$$E_H = \frac{RT}{2F} \ln \frac{p''H_2}{p'H_2} \quad (2)$$

where  $p_{H_2}$  at the left side of the cell and  $p_{O_2}$  at the right side are calculated using the equilibrium constant of the reaction



The electromotive force of the cell represents a stationary one and is equal to

$$E = t_H E_H + t_0 E_0 \quad (4)$$

Current density across the co-ionic electrolyte at a certain point depends on the emf at this point and the terminal voltage  $U$ :

$$j = \frac{E - U}{\rho_{\text{eff}}}, \quad (5)$$

where  $\rho_{\text{eff}}$  is the total resistance of 1 cm<sup>2</sup> of the cell. Partial ion current densities are determined by corresponding electromotive forces as follows from the equations

$$j_H = t_H \frac{E_H - U}{\rho_{\text{eff}}}, \quad (6)$$

\* Corresponding author. Tel.: +30-2421-079065;

fax: +30-2421-079050.

E-mail address: [tsiak@mie.uth.gr](mailto:tsiak@mie.uth.gr) (P. Tsiakaras).

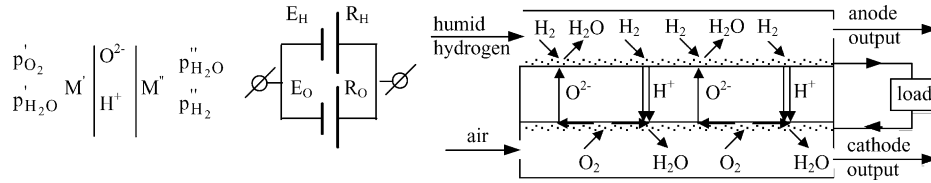


Fig. 1. An electrochemical cell with a co-ionic electrolyte (left), its equivalent circuit (center), and a scheme of a fuel cell based on a co-ionic electrolyte (right).

$$j_0 = t_0 \frac{E_0 - U}{\rho_{\text{eff}}}, \quad (7)$$

Generally,  $E_H \neq E_0$ , so the partial ion currents do not correlate to the transfer numbers. Moreover, the  $U$  value can be between  $E_H$  and  $E_0$  and one of the partial currents can be negative.

In the case of a single cell its efficiency can be calculated by the following equation:

$$\eta = \eta_f \frac{U}{U_{\text{th}}}, \quad (8)$$

where  $\eta_f$  is the fuel utilization,  $U_{\text{th}}$  is the thermoneutral voltage defined as follows

$$U_{\text{th}} = \frac{-\Delta H_{298}^{\circ}}{2F}, \quad (9)$$

where  $\Delta H_{298}^{\circ}$  is the enthalpy of the fuel oxidation reaction. The upper limit of the efficiency is determined by the value of the cell voltage at which the total current density is positive in any point of the cell at a minimum admissible partial pressure of the fuel components in the anode mixture. This voltage value can be called the “maximum admissible voltage”, or simply “maximum voltage” of the fuel cell at such fixed operating parameters as temperature, input fuel gas composition, input air humidity, minimum concentration of fuel components in the anode output gas, and oxygen utilization in the cathode gas (hereafter operating parameters). The maximum voltage can be calculated by the following equation

$$U_{\text{max}} = \frac{t_H(1 - p_{\text{H}_2\text{min}})E_H + t_0 E_0}{1 - t_H p_{\text{H}_2\text{min}}}, \quad (10)$$

where  $p_{\text{H}_2\text{min}}$  is the minimum admissible hydrogen partial pressure in the anode gas. On the whole, the maximum terminal voltage is slightly lower than the cell emf at the inlet.

An important operating performance of the fuel cell is its relative power  $p_r$ , equal to the ratio of its current fuel cell power,  $P$ , to the maximum achievable power (at fixed operating parameters)  $P_{\text{max}}$ :

$$p_r = \frac{P}{P_{\text{max}}}, \quad (11)$$

The fuel cell efficiency is related to the relative power:

$$\eta = 0.5\eta_{\text{max}}(1 + \sqrt{1 - p_r}), \quad (12)$$

where  $\eta_{\text{max}}$  is the upper achievable efficiency at fixed operating parameters. The fuel cell operation at high  $p_r$  when

its voltage is close to half of the emf is unacceptable because of its low efficiency (ca. 50% of the maximum) and, hence, high current losses. The fuel cell operation at low  $p_r$  is attractive from the point of view of high efficiency (and, hence, low current losses) but this is reasonable only when the cost of the fuel cell is low. Development of SOFC technology leads to a reduction of prices of the SOFC units, so analysis of the SOFC operation at high efficiency is important for understanding the potential of SOFCs. One of the acceptable regimes of fuel cell operation is at  $p_r \approx 0.7$ . In this case the fuel cell power can be easily changed (in particular, the power can be rapidly increased by ca. 40%) at the same operating parameters and the fuel cell efficiency in this case is relatively high (ca. 77% of the maximum efficiency).

### 3. Results and discussion

The following operating parameters are accepted in the frame of this paper: the anode input, humid (2%) hydrogen;  $p_{\text{H}_2} = 0.1$  in the anode output; the cathode input, humid (2%) air, the oxygen utilization 0.1; the fuel cell temperature 900 K. It is assumed that  $t_H = t_0 = 0.5$  and do not depend on anode and cathode gas composition. The results are presented for two regimes of the SOFC operation: at maximum terminal voltage and at  $p_r = 0.7$ , and for two modes of the SOFC feeding: co-flow and counter-flow modes. Distributions of parameters are presented for the dimensionless channel, i.e. in coordinates  $x/L$ ,  $L$  the channel length.

In order to demonstrate the special case of the SOFC(O<sup>2-</sup>, H<sup>+</sup>) more clear by the most important characteristics of the SOFC(O<sup>2-</sup>) and of the SOFC(H<sup>+</sup>) for the case of the maximum voltage are shown in Figs. 2–6. Charge transfer and hence the electrical characteristics of the SOFC are determined by the distribution of reactant components along the SOFC channels. Gas mixtures in the fuel cell channels can be described by flow-rates of the gas components and by their partial pressures. Distributions of the anode components partial pressures and their flow-rates expressed as  $N_i/N_{\text{H}_2}(0)$ , where  $N_i$  is flow-rate of  $i$ -component and  $N_{\text{H}_2}(0)$  is hydrogen flow-rate at the inlet, for the case of maximum voltage are plotted in Fig. 2 for the SOFC(O<sup>2-</sup>). It is evident that total gas flow-rate is constant and only redistribution of the partial flow-rates and of the partial pressures of the components occurs in the anode channel. It is possible to show that

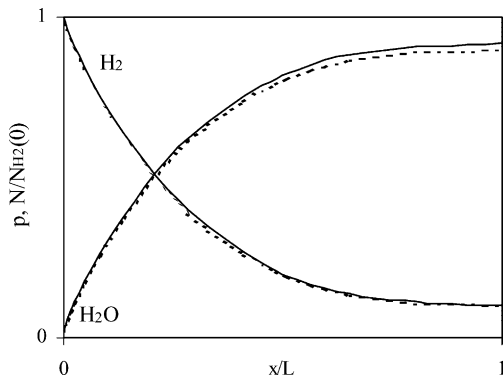


Fig. 2. Distributions of the anode components' relative flow rates (—) and the anode components' partial pressures (---) along the SOFC(O<sub>2</sub><sup>-</sup>). Case of maximum voltage.

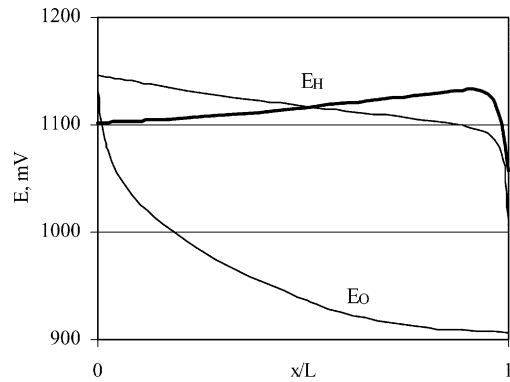


Fig. 5. Distributions of the emf along the SOFC(H<sup>+</sup>) and SOFC(O<sub>2</sub><sup>-</sup>) for the co- (thin lines) and counter-flow (bold line) modes. Case of maximum voltage.

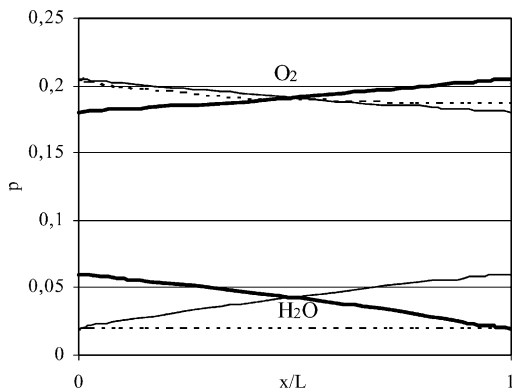


Fig. 3. Distributions of the cathode components' partial pressures along the SOFC(O<sub>2</sub><sup>-</sup>) for the co-flow mode (dashed lines), and along the SOFC(H<sup>+</sup>) for the co-flow (thin lines) and counter-flow (bold lines) modes.

the fuel utilization can be expressed as

$$\eta_f = 1 - \frac{N_{H_2}(L)}{N_{H_2}(0)}, \quad (13)$$

One can see that the fuel utilization in the SOFC(O<sub>2</sub><sup>-</sup>) is about 0.9.

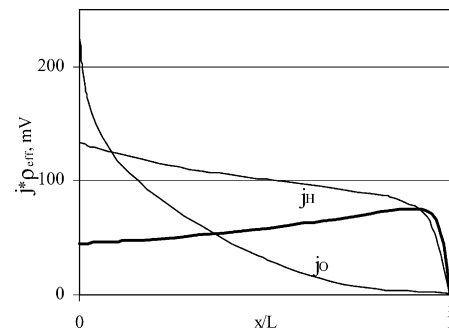


Fig. 6. Distributions of the current densities along the SOFC(H<sup>+</sup>) and SOFC(O<sub>2</sub><sup>-</sup>) for the co- (thin lines) and counter-flow (bold line) modes. Case of maximum voltage.

Distributions of the cathode components' partial pressures are shown in the Fig. 3. In the SOFC(O<sub>2</sub><sup>-</sup>), the oxygen partial pressure changes slightly. The consequence of this is an absence of noticeable dependence of the cathode potential on both the channel coordinate and the mode of the SOFC(O<sub>2</sub><sup>-</sup>) feeding. In the SOFC(H<sup>+</sup>), due to significant relative change of the steam partial pressure, the cathode potential changes considerably from the cathode inlet to the outlet. This causes a noticeable difference in the SOFC(H<sup>+</sup>)

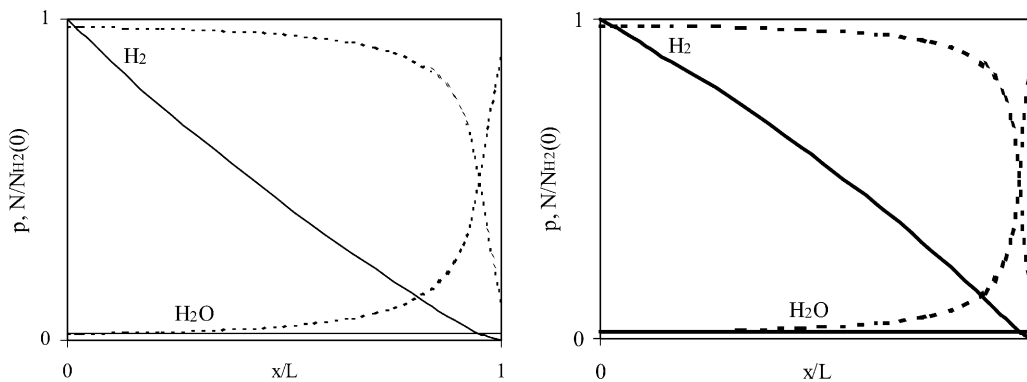


Fig. 4. Distributions of the anode components' relative flow rates (solid lines) and the anode components' partial pressures (dashed lines) along the SOFC(H<sup>+</sup>) for the cases of co-flow (left) and counter-flow (right) modes. Case of maximum voltage.

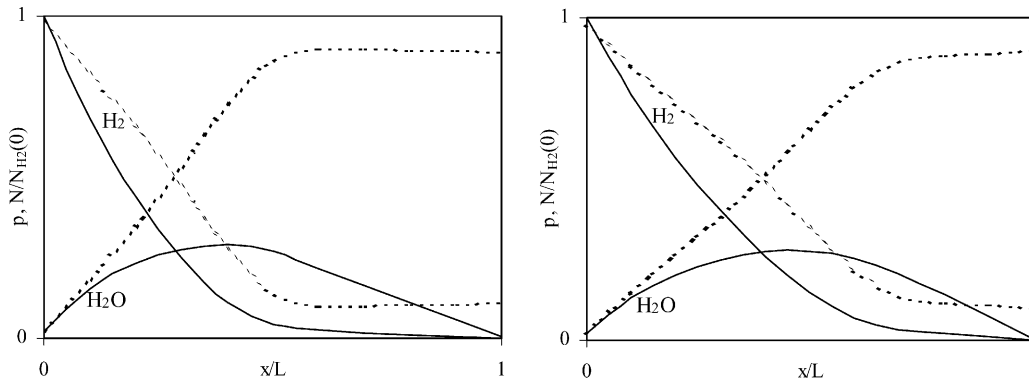


Fig. 7. Distributions as in the Fig. 2 along the SOFC(O<sup>2-</sup>, H<sup>+</sup>) for the co- (left) and counter-flow (right) modes. Case of maximum voltage.

characteristics for different feeding modes. Fig. 4 illustrates the influence of the feeding mode on the characteristics of the anode flow in the SOFC(H<sup>+</sup>). The figures also show that the total anode gas flow-rate decreases from the inlet to the outlet and becomes practically equal to the steam partial flow-rate. One can see that the fuel utilization in the SOFC(H<sup>+</sup>) is very close to 1 in the maximum voltage case.

Fig. 5 demonstrates distributions of the electromotive forces along the two types of the SOFCs. As is mentioned above, the emf distribution in the SOFC(O<sup>2-</sup>) does not depend on the feeding mode. On the contrary, the emf distribution in the SOFC(H<sup>+</sup>) depends strongly on this factor. One of the consequences of this is a difference of the emf at the SOFC(H<sup>+</sup>) outlet for different feeding modes:  $E(L) = 1013$  mV for the co-flow mode and  $E(L) = 1057$  mV for the counter-flow mode. Note that  $E(L) = 909$  mV for the SOFC(O<sup>2-</sup>). It is clear that the terminal cell voltage cannot be higher than  $E(L)$ , so the SOFC(H<sup>+</sup>) has an evident advantage against the SOFC(O<sup>2-</sup>) as regards the possibility to reach higher efficiency, the counter flow mode being more attractive for this purpose.

Distributions of current densities presented in the form  $j\rho_{\text{eff}}$  are shown in Fig. 6. A strong irregularity of the current density in the SOFC(O<sup>2-</sup>) causes significant thermal stresses due to the irregularity of heat-evolution. The current density

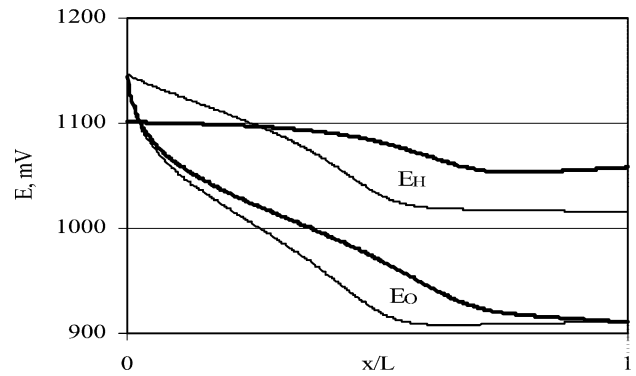


Fig. 8. Distributions of the electromotive forces corresponding to various charge carriers along the SOFC(O<sup>2-</sup>, H<sup>+</sup>) for the co- (thin lines) and counter-flow (bold lines) modes. Case of maximum voltage.

within most of the SOFC(H<sup>+</sup>) changes considerably less than in the previous case. Numerical integration allows us to find an average current per unit of the SOFC area,  $j_{\text{av}}$ , and consequently an average specific SOFC power,  $P_{\text{av}}$ ,

$$P_{\text{av}} = j_{\text{av}}U = \frac{(E_{\text{av}} - U)U}{\rho_{\text{eff}}}, \quad (14)$$

Figs. 7–9 illustrate characteristics of the SOFC(O<sup>2-</sup>, H<sup>+</sup>) for the maximum voltage case. The total anode flow-rate as

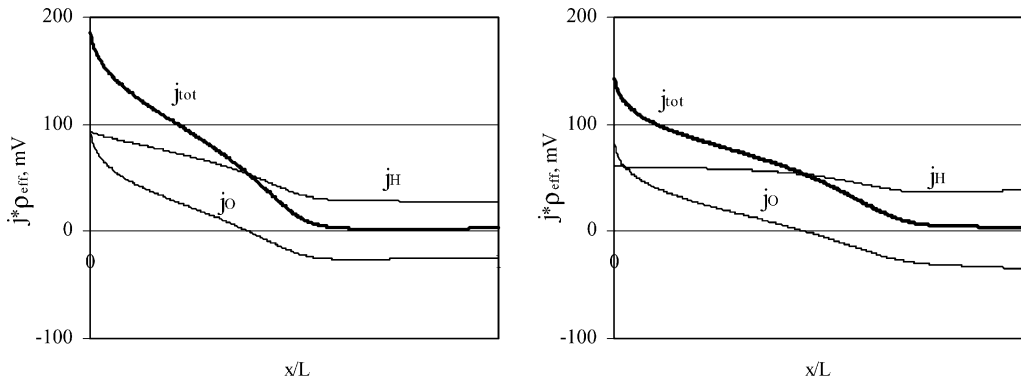


Fig. 9. Distributions of the current densities along the SOFC(O<sup>2-</sup>, H<sup>+</sup>) for the co-flow (left) and counter-flow (right) modes. Case of maximum voltage.

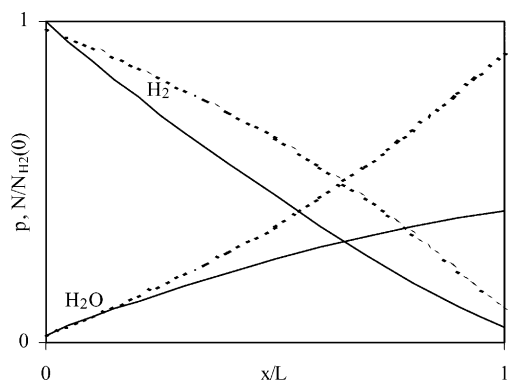


Fig. 10. Distributions as in Fig. 2 along the SOFC(O<sup>2-</sup>, H<sup>+</sup>). Case of  $p_r = 0.7$ .

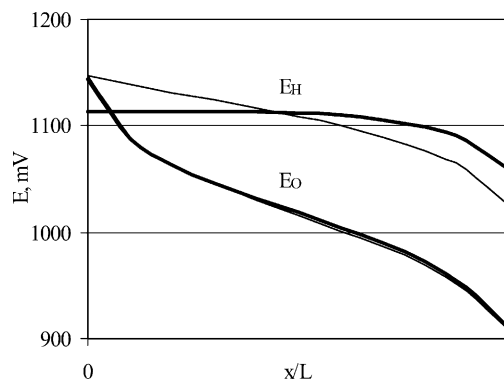


Fig. 11. Distributions as in Fig. 8. Case of  $p_r = 0.7$ .

well as the hydrogen flow-rate slow down gradually practically to zero at the end of the channel while the steam flow-rate reaction reaches a maximum (Fig. 7). The hydrogen partial pressure reaches a minimum value at the end of the channel in the case of the counter-flow mode, while, in the case of the co-flow mode, it has a minimum approximately in the middle of the channel and then rises slightly. It is necessary to point out that neither the operating regime, nor the terminal voltage affect noticeably the nature of the distributions of the cathode components and they are practically the same as is reported in Fig. 3.

Fig. 8 demonstrates distributions of the electromotive forces corresponding to various charge carriers. The values

of the emf at the end of the cell differ considerably. As is mentioned above, the terminal voltage can be between these values:  $E_0(L) < U < E_H(L)$ . In this case, the oxygen ion current density is negative while the total current density is positive (see Fig. 9). Of course, a substantial part of the cell generates an insignificant part of the cell power and could be eliminated, but this would lead to a lowering of the fuel utilization and hence to a lowering of the efficiency. On the whole, the current density is very irregular, although the counter-flow mode is more favourable.

Characteristics of the SOFC(O<sup>2-</sup>, H<sup>+</sup>) at  $p_r = 0.7$  are shown in Figs. 10–12. An increase of the relative power, i.e. a decrease of the terminal voltage, influences strongly all the cell characteristics. One can see, in particular, a decrease of

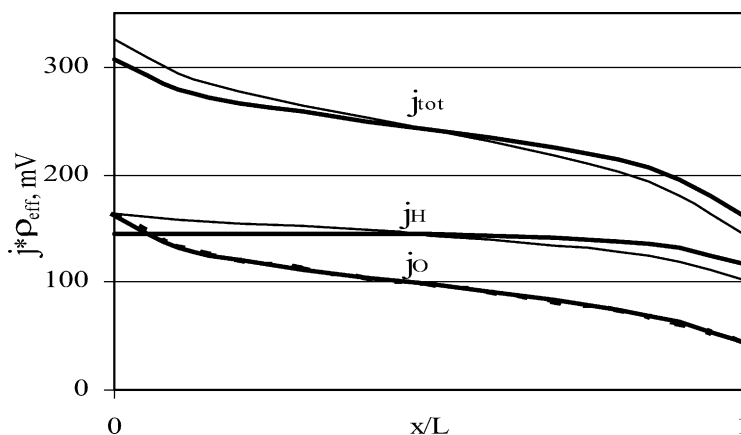


Fig. 12. Distributions of the current densities along the SOFC(O<sup>2-</sup>, H<sup>+</sup>) for the co-flow (thin lines) and counter-flow (bold lines) modes. Case of  $p_r = 0.7$ .

Table 1  
The main characteristics of the SOFC(O<sup>2-</sup>, H<sup>+</sup>) in comparison with the SOFC(O<sup>2-</sup>) and the SOFC(H<sup>+</sup>)

$T_H$	Feeding mode	Case of the maximum voltage				Case of $p_r = 0.7$			
		$\rho_{\text{eff}} P_{\text{av}}$ (mV)	$\eta_f$	$U$ (mV)	$\eta$	$\rho_{\text{eff}} P_{\text{av}}$ (mV)	$\eta_f$	$U$ (mV)	$\eta$
0	Co-flow	88.1	0.9	908	0.650	333.6	0.900	777	0.556
0.5	Co-flow	91.0	$\approx 1$	960	0.766	393.2	0.954	821	0.625
	Counter-flow	94.0	$\approx 1$	980	0.782	394.4	0.954	822	0.626
1	Co-flow	201.8	$\approx 1$	1012	0.807	434.5	0.998	865	0.689
	Counter-flow	123.2	$\approx 1$	1057	0.842	436.0	0.998	865	0.689

the terminal voltage leads to a decrease of the fuel utilization (Fig. 10), to an increase of the emf values (Fig. 11), and to an increase of the current density values and to their higher uniformity (Fig. 12).

The most important characteristics of the SOFC, such as the terminal voltage, the average specific power calculated according Eq. (14), the fuel utilization, and the efficiency are presented in the Table 1 for the SOFC(O<sup>2-</sup>, H<sup>+</sup>) in comparison with the SOFC(O<sup>2-</sup>) and the SOFC(H<sup>+</sup>). One can see that the higher proton transfer number the higher the SOFC efficiency. Increase of the terminal voltage also leads to a noticeable increase of the SOFC efficiency, however, this leads to a considerable decrease of the SOFC specific power.

#### 4. Conclusions

The analysis presented shows that the SOFC based on the co-ionic electrolyte has significant advantages over the SOFC based on the oxygen ion electrolyte and very

close to the efficiency of the SOFC based on the proton electrolyte when they operate at the relative power of 0.7. The SOFC(O<sup>2-</sup>, H<sup>+</sup>) efficiency is very high when it operates at maximum power, but the specific power in this case is significantly lower. The main aim in SOFC technology must be the elaboration of a cheap and stable co-ionic electrolyte with as high proton transfer number as possible.

#### Acknowledgements

This work was supported by INTAS99 (#897).

#### References

- [1] H. Iwahara, T. Yajima, T. Hibino, K. Ozaka, H. Suzuki, SSI 61 (1993) 65.
- [2] N.V. Arestova, *Electrochimia* (Russian) 30 (1994) 998.
- [3] N. Bonanos, K.S. Knight, B. Ellis, SSI 79 (1995) 161.
- [4] A. Demin, P. Tsiakaras, *Int. J. Hydrogen Energy* 26 (2001) 1103.